Journal of Solid State Chemistry 183 (2010) 2786–2796

Contents lists available at ScienceDirect

Journal of Solid State Chemistry

journal homepage: www.elsevier.com/locate/jssc

Water solubility in calcium aluminosilicate glasses investigated by first principles techniques

Frédéric Bouyer [a,*], Grégory Geneste [b], Simona Ispas [c], Walter Kob [c], Patrick Ganster [d]

[a] Laboratoire d'étude du Comportement à Long Terme, Commissariat à l'Énergie Atomique et aux Énergies Alternatives, Centre de Marcoule, SECM - LCLT, BP 17171, 30207 Bagnols-sur-Cèze Cedex, France
[b] CEA, DAM, DIF, F-91297 Arpajon, France
[c] Laboratoire des Colloides, Verres et Nanomatériaux, UMR CNRS-UM2 5587, Université Montpellier II, Place Eugène Bataillon, 34095 Montpellier Cedex 5, France
[d] Centre SMS, UMR CNRS 5146, École des Mines de Saint-Etienne, 158 cours Fauriel, 42023 Saint-Etienne Cedex 2, France

ARTICLE INFO

Article history:
Received 17 March 2010
Received in revised form
20 July 2010
Accepted 25 August 2010
Available online 21 September 2010

Keywords:
Glass leaching
Reactivity in glass
Aluminosilicate
Hydrolysis
First-principles calculations
SIESTA

ABSTRACT

First-principles techniques have been employed to study the reactivity of water into a calcium aluminosilicate glass. In addition to the well known hydrolysis reactions $Si{-}O{-}Si + H_2O \rightarrow Si{-}OH + Si{-}OH$ and $Si{-}O{-}Al + H_2O \rightarrow Si{-}OH + Al{-}OH$, a peculiar mechanism is found, leading to the formation of an AlO_3–H_2O entity and the breaking of Al–O–Si bond. In the glass bulk, most of the hydrolysis reactions are endothermic. Only a few regular sites are found reactive (*i.e.* in association with an exothermic reaction), and in that case, the hydrolysis reaction leads to a decrease of the local disorder in the amorphous vitreous network. Afterwards, we suggest that ionic charge compensators transform into network modifiers when hydrolysis occurs, according to a global process firstly suggested by Burnham in 1975. Our theoretical computations provide a more general model of the first hydrolysis steps that could help to understand experimental data and water speciation in glasses.

1. Introduction

Chemical interactions between water and minerals or glasses is a subject of investigations in many fields, from solid state physical chemistry to geochemistry, and cover several interests, from fundamental science to industrial applications; one of the major application is the improvement and the insurance of nuclear wastes storage [1–7]. In addition to a very large community interest and the growing progress of experimental apparatus over a very large scale (from macroscopic- to the nano-scales), some fundamental mechanisms need to be clarified and especially dissolution processes of such materials at the atomic scale.

The water–silicate interaction (simple silica as well as alkaline silicate glasses) has been firstly described more than twenty years ago [8,9] by the simple hydrolysis reaction of Si–O–Si (siloxane species) into two Si–OH (silanols) groups, using small clusters such as H_3Si–O–SiH_3 aggregate (disiloxale molecule) without any environment and by means of quantum chemistry principles. The energetic change of the reaction $Si{-}O{-}Si + H_2O \rightarrow 2Si{-}OH$ was found to be close to zero [8], slightly endothermic to be precise (+0.09 eV). These first calculations highlight that a small increase of the Si–O bond (4%) is sufficient to switch the balance of the energy reaction to make it exothermic. Even if these first studies have been investigated on small clusters and did not take into account the condensed matter character of the amorphous solid, these pioneering works underline a specific character of the siloxanes bond hydrolysis reactions: the formation of the silanols groups is not associated to a clear energetic trend or, from a chemical point of view, is not a strong thermochemical reaction. The energy reaction may be influenced by the near environment and the deformation of the local geometric bonds. From a cluster to an other, or more, from system to system, the Si–O–Si bond hydrolysis may be endothermic or exothermic depending to the short-range or middle-range local structure disorder surrounding the considered siloxane bond. However, the energy barrier for such a reaction is relatively high, and typically exceeds 1 eV.

In bulk amorphous SiO_2, however, Bakos [10] studied the diffusion of water and hydrolysis of the siloxane bonds. A 0.8 eV barrier was found for migration through 6-membered rings, and a ≈ 1.5 eV activation energy for hydrolysis reactions, found to be endoenergetic in all the computed cases ($\Delta E \approx +0.3$ to 0.7 eV). Anyway these results do not explain the speciation of water observed in the bulk of silica and alkaline silicates [11–15] at high pressure and temperature (80–800 °C). According to a number of experiments, under specific conditions, molecular water transforms in the bulk into silanol groups at low water content, suggesting that a number of siloxane bonds have been hydrolyzed. When the water content increases, the silanol concentration saturates and stable

---

[*] Corresponding author.
E-mail address: frederic.bouyer@cea.fr (F. Bouyer).

0022-4596/$ - see front matter © 2010 Elsevier Inc. All rights reserved.
doi:10.1016/j.jssc.2010.08.031

molecular water appears in the glass, as shown by IR experiments. The same trend, anyway, is found in aluminosilicate glasses [16] and seems therefore to be a common property of various glasses.

In this paper we focus on more complex calcium aluminosilicate glasses, and their reaction with water in bulk. Calcium aluminosilicates are materials of interest, present in the nature under various crystalline forms, either pure (anorthite) or hydrated (bicchulite, chantalite, clinozoisite…). Moreover, in their amorphous state, these materials constitute the skeleton of the so-called "gel" or alteration glass layer, that forms at the surface of the nuclear waste storage matrices when they are put in contact with water. Their reactivity with respect to water is therefore a crucial point, that needs to be clearly understood to ensure the long-term durability of the nuclear waste storage, since water is one of the most corrosive substance for silicate materials in the nature. Unfortunately, the molecular mechanisms acting in glass leaching are not clearly explained at the present time, even though they are now clearly identified [17,1]. We focus in this paper on the hydrolysis mechanisms, that lead to a *depolymerization* of the glass network. The interdiffusion of alkaline species with protons or hydronium ions [18–28] is a complementary process of glass leaching that will not be dealt with in this paper.

The molecular mechanisms at the root of the speciation and diffusion of water in hydrated aluminosilicate glasses and melts (especially albite) have also been a subject of many investigations over the past 20 years [29–33]. Among the possible reactions, beside the hydrolysis phenomena $T{-}O{-}T'+H_2O \rightarrow T{-}OH+T'{-}OH$ (T, $T'=$ Si or Al) (see the review by [33], one sometimes mentions the possible dissociation of water against the network modifiers (Na in the case of albite) Na^+ (Al–O–Si) + $H_2O \rightarrow H^+$(Al–O–Si) + NaOH, that would give rise to a bridging hydroxyl and to an hypothetical NaOH entity, never observed to our knowledge in glasses under the form of a triatomic molecule. This mechanism had already been severely criticized by Doremus a long time ago [34]. It seems that hydrated aluminosilicates do not contain Al–OH groups but contain Si–OH (silanol) species and are characterized by a specific vibration mode at $\approx 900\,cm^{-1}$. The NMR measurements of Oglesby and Stebbins [35] suggest the presence of silanol groups and protonated aluminosiloxane bonds Al–OH–Si (bridging hydroxyls). The ab initio calculations performed by Liu et al. [36] also suggest that both entities must coexist in hydrated aluminosilicates to explain the NMR measurements. Finally Kubicki and Sykes [37] come to the same conclusion and attribute the $900\,cm^{-1}$ mode to a peculiar vibration mode of the Al–OH–Si group (protonated bond).

Thus, if the nature of the chemical species present in hydrated aluminosilicate glasses is quite well understood, the molecular mechanisms that lead to their formation, their stability and probability to form is not well known at the present time. Our aim in this article is (1) to describe the possible reactions of water with a calcium aluminosilicate ("CAS") glass in bulk and to characterize as much as possible the chemical products of such reactions, and (2) to provide a simple model that helps to understand the first steps of glass leaching in a general way (*i.e.* extended to various kinds of glasses). After giving some details about the numerical method in Section 2, we describe in Section 3 a set of possible reactions in bulk, first in the case of a chemical reaction of water with the siloxane bonds, then in the case of a reaction with Al sites. In the same Section, results are discussed in each (Section 3.2 and 3.4) and a general model for the first steps of the hydration of glasses is suggested.

2. Computational elements

The interaction between all atoms, water and glass in bulk, is investigated on a 100-atom sample periodically repeated in the 3 dimensions to model the extended bulk glass. The composition of the studied glass (67% SiO_2, 12% Al_2O_3, 21% CaO) is a simplified composition of a gel of French R7T7 nuclear glass [5,2,4,3,1,6,7]. This sample can be viewed to model the so-called gel, resulting from the alteration of the glass into the water. The sample studied, taken from the work of Ganster [38,39], has been generated by quenching a melt previously equilibrated at high temperature within classical interatomic potentials (the same as those used in Ref. [39]). Ganster et al. [39] showed that such a size is enough to avoid the unphysical finite-size effects that can be generated by the periodic boundary conditions. The supercell volume is fixed to reproduce the density of the real gel.

After a short time of ab initio molecular dynamics (0.5 ps), the geometry of the whole sample is optimized by using the ab initio tool (the SIESTA[1] code [40–42]), by minimizing the total energy until the maximum component of the atomic forces is lower than 0.04 eV/Å, ensuring an accuracy better than 0.01 eV on total energies and better than 0.01 Å on interatomic distances. All the calculations are performed in the framework of the density functional theory (DFT) [43]. We use the SIESTA code [40,41] and the Generalized Gradient Approximation of Becke [44], Lee et al. [45] for the exchange-correlation energy. The periodic parts of the Kohn–Sham wave functions are expanded on a numerical atomic orbital basis set including double zeta and polarization orbitals. The effect of core electrons (1*s*, 2*s* and 2*p* for Si and Al, 1*s* for O, 1*s*, 2*s*, 2*p*, 3*s* and 3*p* for Ca) is accounted for through the use of Troullier–Martins pseudopotentials [46,47]. On the one hand, the geometry optimizations are performed without using the spin degrees of freedom in the self-consistent resolution of the Kohn–Sham equations, consistently with the non-magnetic character of such materials. On the other hand, the molecular dynamics computations are performed by taking into account the spin of each element, so that the energies barriers during the dynamics reactions pathways are not overestimated.

Since it is obviously impossible to simulate hydrolysis events with a sufficient occurrence through ab initio molecular dynamics (the activation barrier is much too high—typically 1 eV), the reactivity of a given bridging bond is investigated by starting from an initial guess for the configuration in which the bond is hydrolized, and making the whole system relax until the above mentioned criterion on maximal forces is achieved. In other words, we force the bond to be broken and let evolve the system to the final product. In a number of cases, the stability of the resulting relaxed system has been tested by performing ab initio molecular dynamics at high temperature (1000 K) (on 0.5–2 ps), at which the quantum effects related to the stretching vibration modes of OH groups can be considered as negligible. In some cases, interesting elementary mechanisms involving exchanges and diffusion of protons were observed. In addition of these chemical interpretations, this type of computation suggests that the final local optimum of the system is reached, *i.e.* the products are obtained in a thermochemical point of view.

All the calculations are performed under constant volume. The over-pressure (or stress) induced by incorporating one H_2O molecule in our glass system can be considered as negligible since the over-pressure calculated during ab initio dynamics (through the temperature and atomic motions) is clearly above. Thus the species found and determined through ab initio computations cannot be considered as an artefact of the methodology used for describing the system of interest. Furthermore, the vibrational structure is calculated in various cases through a finite-difference algorithm and the density of vibration modes projected on the hydrogen atoms when necessary.

---

[1] See: http://www.uam.es/siesta

Finally we would like to underline that electronic structure calculations are both a very powerful technique but also a limited tool. They allow to describe with a nice accuracy very subtle mechanisms occurring at the atomic scale. They give a precise description of chemical bonds and electron transfers, and reproduce quite well the vibrational structure in various systems. But one must keep in mind that (1) the calculations are always performed in the framework of an approximation (GGA-BLYP in our case) and (2) the heavy computational cost of the method prevents from having access to any statistical dimension, at the opposite of what can be done within empirical potentials. This work thus constitutes a first step of a wider theoretical study of glass leaching. Besides these limitations just explained above, we would like to mention that the use of pseudopotentials have been previously validated [21,48] on small systems, as well as on the free enthalpies of reactions (as a function of temperature) which is out of the scoop our this paper. The GGA exchange and correlation functionals used for all calculations [44,45] correctly reproduce crystallographic structures, enthalpies, entropies and free enthalpies of SiO_2 (as functions as the temperature, that is by applying thermochemical statistics concepts using vibrational analyses) and all its allotropic structures ($\alpha-$quartz, $\beta-$quartz, $\alpha-$cristobalite, Al_2O_3-α, kaolinite phases). The GGA exchange-correlation energy is the best functional to apply on our systems, since it takes into account the gradient of the density: $E_{xc}[\rho] = \int \rho(r)\varepsilon_{xc}[\rho(r),|\nabla\rho(r)|]\,dr$, and is adapted to reproduce all electronic density variations on the whole system (iono-covalent bonds), compared to the local density approximation which is the best approach to handle large homogeneous electronic density systems (typically metallic systems).

3. Hydrolysis in the glass bulk

3.1. Review of published theoretical and experimental data

Water diffusion into the glass has been analyzed by Bunker [17]. As mechanisms explaining molecular glass corrosion, he proposed two reaction pathways for water introduction into pure silicate glass. For 6-membered rings, water penetration occurs by diffusion (molecular diffusion), whereas for smaller rings, water gets forward in the glass bulk by hydrolysis mechanism. These experimental results are in good agreement with theoretical computations: Bakos et al. [10] pointed out that water diffusion needs an energy around 0.8 eV to diffuse across a 6-membered rings. Furthermore, they found that hydrolysis mechanisms have a 1.5 eV activation energy for endothermic reactions (whose reactions energies are between +0.3 and +0.7 eV). Anyway all these results cannot explain the speciation of water observed at high temperature and pressure (from 80 to 1000 °C). According to a collection of experiments (see for instance: [11–15]), molecular water reacts with the glass bulk to form silanol (Si–OH) groups at low water content. This suggests that a number of siloxane bonds have been hydrolyzed. When the water content increases, experimental Infra-Red studies show stable molecular water into the bulk after saturating silanol groups by hydrolysis. The same result has been observed in albitic glasses [16] and suggests to be a common trend and a general property in various silicate and aluminosilicate glasses.

3.2. Si–O–Si bonds hydrolyses in the glass bulk: reactivity of siloxanes bonds

First, we focus on all the Si–O–Si bonds that can be hydrolyzed in our 100-atom sample, as described in (2). The hydrolysis reaction:

$$Si-O-Si+H_2O \rightarrow Si-OH+Si-OH \qquad (1)$$

has been simulated by starting from an initial guess (a broken bond) and by allowing this starting configuration to stabilize by the conjugate gradient method implemented in the SIESTA code. All configurations have been generated in the same way, by breaking one by one all possible covalent Si–O–Si bridges. Results are disparate, both in term of final configurations obtained and of energy reactions calculated. The amorphous character of the glass and the neighborhood of the hydrolyzed site seem to play an important role on the reactivity with water. Nevertheless, we can classify the final geometric configurations into two essential groups.

- The two silanol groups evolved towards the (a) configuration (see Fig. 1) in which they roughly remain equivalent; in fact, the chemical Si–O–Si bonds are not really broken: two bridging hydroxyls Si–OH–Si appear, with an interatomic distance between the two Si less than 4 Å. The Si–O–Si bond is not hydrolyzed and the final configuration is quite symmetric. The (a′) configuration refers to a non-hydrolyzed Si–O–Si site too, with a bond length less than 4 Å. It suggests that the near neighborhood induces a small stress on that site and prevents to be hydrolyzed. Both (a) and (a′) configurations are the result of endothermic processes, and the Si–Si interatomic distance is almost not changed compared to the initial state.
- In a small number of cases (three sites within the 100-atom sample), the initial state evolves to a much more stable configuration, with two silanol groups bridged by and hydrogen bond, that probably stabilizes the whole system. These non-symmetric configurations are illustrated by the Si–Si interatomic distance which is stretched to about 4 Å and sometimes larger.

To get more insight into the calculated configurations presented above, we now focus on the vibrational frequencies computed on both systems (a) and (b). This type of calculations has been done using SIESTA and finite differences to estimate the energy gradients on both configurations. All frequencies were above 0, which proves that these configurations are correctly optimized and correspond to a local minimum of the energy surface of the system.

Configuration (a):	*symmetric configurations*. The configurations we analyzed correspond to the ones depicted in the Fig. 1(a) (configuration (a) or (a′)). The vibrational density of states (see Fig. 2(a)) has been projected on the H atoms, so that only H contributions can be highlighted: the four highest frequency modes are shown on Fig. 4(a) and correspond to the projected density of vibrations depicted on Fig. 3(a). These modes correspond to OH stretching modes, those frequencies are in the range of 3000–3400 cm^{-1}, and the others refer to OH bending modes, whose frequencies are around 1000–1100 cm^{-1}. As pointed out previously, all configurations have an higher energy (they are less stable) compared to the initial configuration (that is: glass dry plus a water molecule), of about 2 eV.
Configuration (b):	*non-symmetric configurations*. Fig. 1(b) (configuration (b)) shows the final optimized system for which normal modes and frequencies were calculated. The density of vibrations (Fig. 2(b)) has been projected on H atoms of the sample for obtaining the only H contributions (Fig. 3(b)).

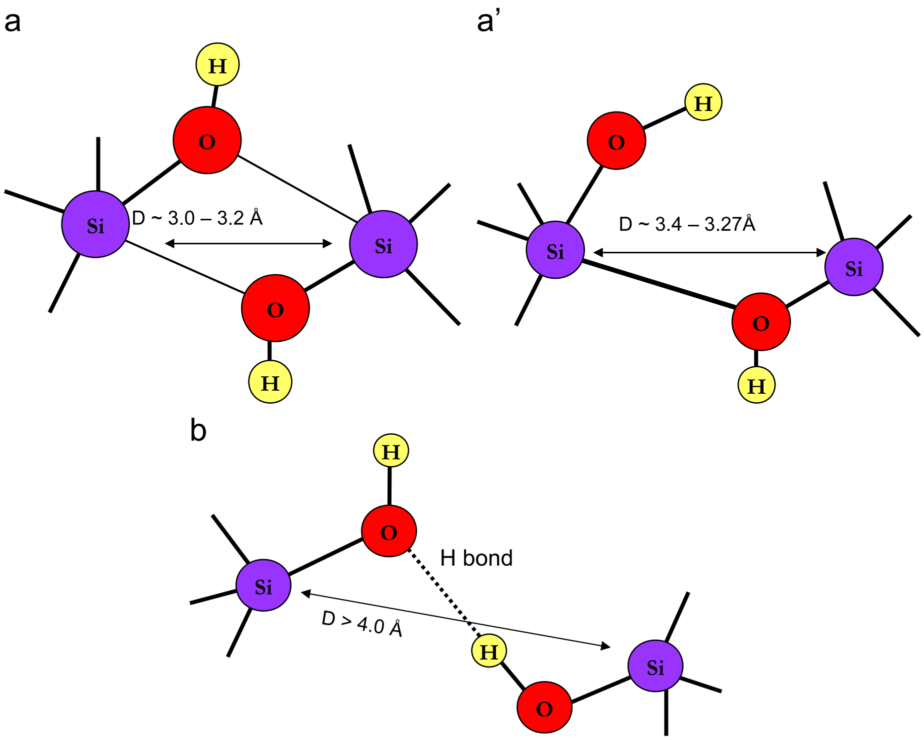

Fig. 1. The two types of configurations calculated after hydrolysis of siloxane Si–O–Si bonds. (a) and (a′) illustrate endothermic reactions and (b) illustrates silanols bonded and stabilized by an H-bond.

Two silanol groups appear, bridged to each other by H bonds, as depicted on Figs. 1 and 4(b). In that configuration, two highest frequency modes are clearly separated, and splitted (if we consider that in Fig. 3(a) the highest frequencies are almost degenerated for the configuration (a)), and correspond to the OH bonds stretchings of the hydroxyls. They appear around ~3160 and 2060 cm^{-1}. The softer mode (2060 cm^{-1}) corresponds to the hydrolyl for which the H atom is engaged into the hydrogen bond. This kind of H-bond is well known to soften stretching modes of hydroxyl groups [14]. Two bending modes localized at 1240 and 1400 cm^{-1} correspond to a combination of each H atom perpendicular of the OH-bond: they reveal a strong dynamic coupling between hydroxyls groups. The final Si-Si distance is widely open by more than 1 Å after the optimization of the process: OH-bonds can turn themselves to bind to each other with the formation of H-bond. In the near environment, the whole structure of the glass is fully relaxed. The reaction process is exothermic; only three sites of this type have been found in the studied sample.

3.3. Model and discussions on the processes reactivity of Si–O–Si

In the final configuration, the interaction between silanols groups probably plays an important role on the reaction energy. First of all, we would like to estimate the total energy contribution of this interaction by computing several configurations of two small H_3 Si–OH molecules separated by a given Si–Si distance (which is fixed in our calculations).

Two configurations may exist: one which is "symmetric" (see Fig. 6) with two equivalent groups, one "non-symmetric" (see also Fig. 6) for which the two groups are bridged by an H-bond. If the Si-Si distance is less than 4 Å, only the symmetric configuration is stable whereas the other asymmetric system becomes more stable if the Si-Si distance is increasing, exceeding 4 Å. These two "symmetric" and "non-symmetric" configurations are the ones calculated into the glass bulk, and presented above (see Section 3.2), and correspond to the (a) and (b) configurations (Fig. 1).

All these results suggest that there is a limited number of sites that are reactive with water in the bulk of the glass. One possible origin (reason) on the reactivity increase might be the internal stress. In the studied sample, the stress is not zero, since the atomic density is fixed to reproduce the experimental one. This quantity reflects a macroscopic stress, that cannot be separated into local individual contributions at an atomic scale. Rather than considering an internal stress effect, the selective reactivity is probably coming from the degree of structural disorder in the near neighborhood of the considered site. Fig. 5 shows the standard deviation of the Si–O–Si angle distribution, for optimized configurations (that is, after reaction with water), as a function of the energy for each fully optimized geometry. The whole distribution is centered on the ~109° value; in the case of exothermic reactions, the distribution is much more closed to this ideal value (109°) with a sharper standard deviation (around 6–7°), whereas endothermic reactions lead to a wider range of standard deviation (8–10°). There is a correlation between reactivity and the short-range structural order around a selected site, that can explain the selective reactivity in amorphous system. In fact, all sites are not equivalent in this non-crystalline object, and thus offer a different affinity to hydrolysis due to local order in the near neighborhood. The effect of a mid-range disorder is very difficult to investigate due to lack of statistics but could certainly play a role in the chemical processes within the whole glass.

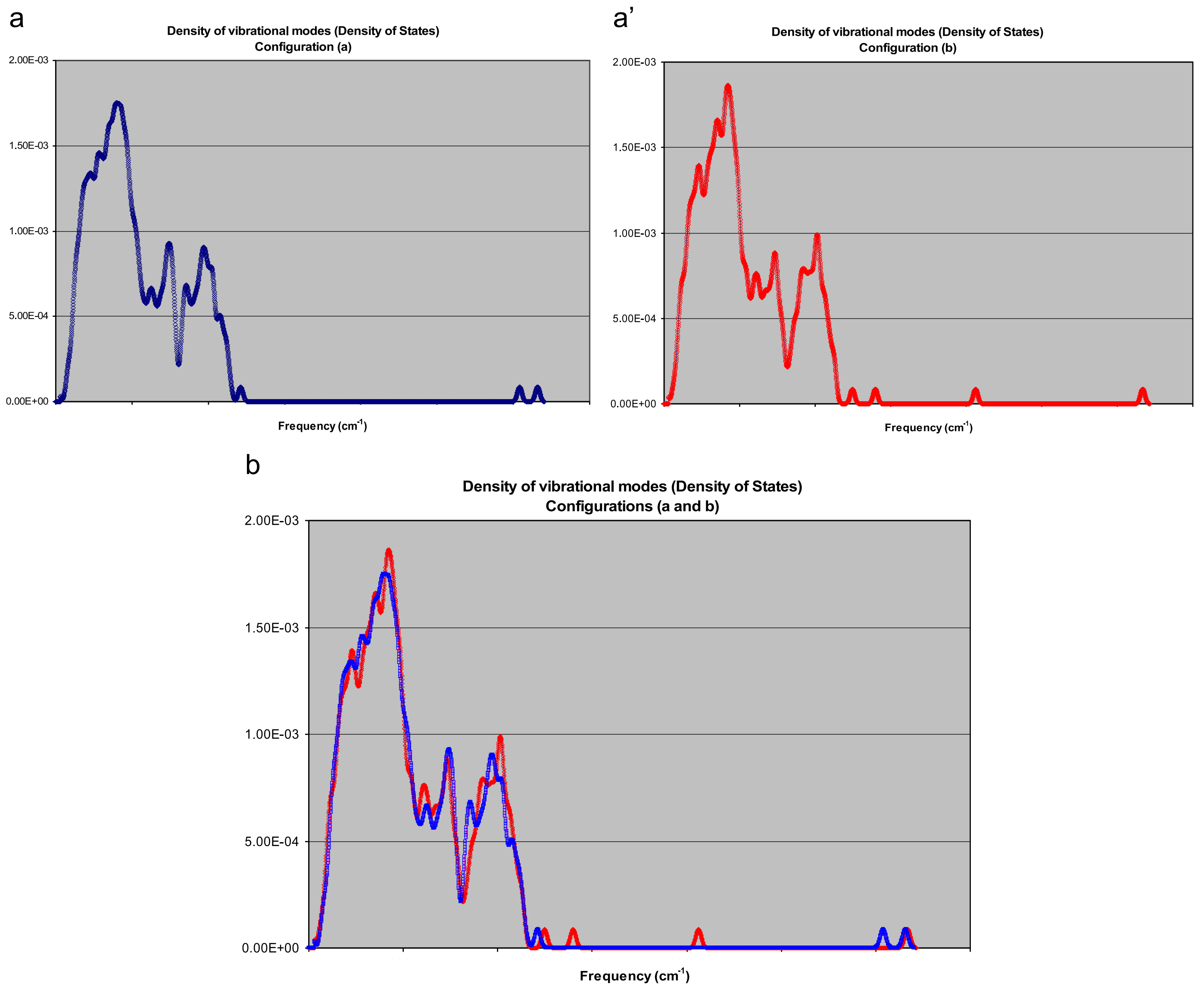

Fig. 2. Density of vibrational modes (density of states) for both configurations (a) and (b) (see Fig. 1).

Accordingly, we highlight that glass is inhomogeneous in terms of reactivity, and specific chemically reactive sites are related to the vitreous structure which is responsible to "active" sites. This typical reactivity trend has been observed through IR measurements in glasses (such as aluminosilicates [16] and alkaline silicates [11,12]) in contact with vapor water at high temperature and high pressure. In fact, at low water content, observations show that water is dissociated into silanols –Si–OH, and no molecular water is found. On the other side, when water content increases, the chemically "active" sites (exoenergetic hydrolysis) are fewer and fewer until there is no more reactive site, and the hydroxyl group concentration saturates in the glass. Then, molecular water appears and increases linearly with the water content. All these observations are in good agreement with the interpretations of our computational studies. The equilibrium constant of the hydrolysis chemical reaction must be reviewed in order to take into account the two following key points:

- first, the two silanols groups are not independent, and as suggested by Oehler and Tomozawa [15], it is more appropriate and accurate to explicitly take into account "silanols pairs" in the hydrolysis process:

$$\mathrm{Si{-}O{-}Si + H_2O \leftrightarrow (Si{-}OH)_2} \quad (2)$$

- second, a few sites –Si–O–Si– are reactive. If we consider, as suggested by the present study and corroborated by Oehler and Tomozawa [15], that all siloxane bonds have not the same affinity to react with water, and that only of a certain fixed number N_0 of siloxane groups per unit of volume is reactive, we have to take in consideration their chemical activity in the chemical K constant. With the following notation:
    - ◦ S: the concentration of silanols pairs $(\mathrm{Si{-}OH})_2$
    - ◦ W: the concentration of water molecule
    - ◦ N: the concentration of the remaining "active" sites, we have also: $N_0 = N + S$

we have the relation:

$$K = \frac{[(\mathrm{Si{-}OH})_2]}{[\mathrm{H_2O}]\cdot N} = \frac{S}{W\cdot(N_0 - S)} \quad (3)$$

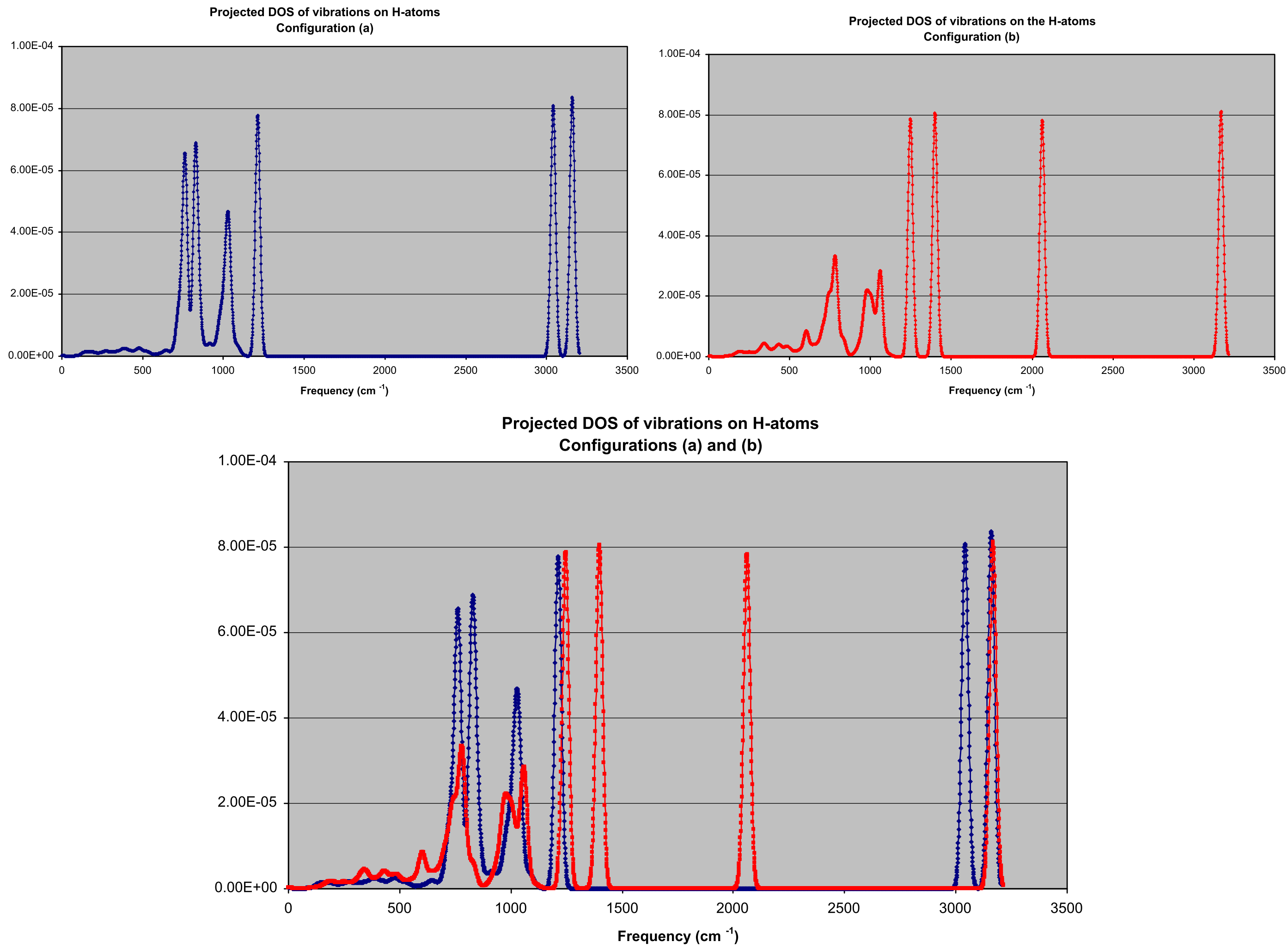

Fig. 3. Projected density of state (DOS) of vibrations projected oh the H atoms of the sample. Both configurations (a) and (b) are presented.

All concentrations are assumed to be uniform within the whole sample, and without any kinetics, that is the chemical equilibrium is supposed to be reached. The total water content introduced into the glass is then $T=W+S$. It is fairly straightforward to obtain the following equation, for which S is solution:

$$K=\frac{S}{(T-S)(N_0-S)}$$

Rewriting this equation in lowercase by normalizing all quantities (dimensionless numbers $s=S/N_0$ and $t=T/N_0$), we obtain for s a function of the normalized total water content t:

$$s(t)=\frac{1}{2}\left(1+t+b-\sqrt{(1+t+b)^2-4t}\right),\quad b=\frac{1}{K.N_0},\quad w(t)=t-s(t). \qquad (4)$$

A simple numerical application is shown on Fig. 7 with $b=0.04$. This simple model, based on our assumptions suggested by our computational studies, correctly qualitatively describes the experimental observations reported in Refs. [11,12,16].

3.4. *Si–O–Al bonds hydrolysis: reactivity of Al–O–Si bonds and $(AlO_4)^-$ sites*

As well as for siloxanes bonds, similar calculations have been performed on Al–O–Si bonds, and the same trend concerning hydrolysis (exo- and endo-energetic sites) has been confirmed by our computations. Furthermore, at some sites, another chemical species has been found, as a result coming from the reactivity of water on Al.

In a number of Al sites, water reacts immediately and binds directly onto Al while the Al–O–Si bond (or Al–O–Al bridge, whose case is very seldom, but present in our sample) is broken concomitantly, like a “concerted” reaction from a chemical point of view. It leads to a chemical species $-AlO_3-H_2O$ as depicted on Fig. 8. The available oxygen atom forms a new bond with an available Ca atom close to the tetrahedron. The new formed bond $-Al-O-H_2$ is perpendicular to the—(AlO_3) plane; moreover, the bond length is relatively short, between 1.8 and 1.9 Å. It proves that this bond is not a simple physisorption, but leads to a new strong bond resulting from an effective chemical reaction. This process is spontaneous with a reaction energy decrease of about 0.6–0.7 eV (thus thermochemically more stable). The vibrational modes have been computed on one optimized configuration (Fig. 9). The density of states of the vibrational analysis projected on the H atoms is depicted on Fig. 10. It underlines four most important vibrations: the three highest frequencies are those of the classical stretching and bending modes of molecular water, except the symmetric and asymmetric stretching modes of H_2O that are changed into two separated –OH stretching vibrations. The new 810 cm^{-1} mode is much more peculiar and correspond to a rotation or a “rocking” motion around the Al–O bond. This

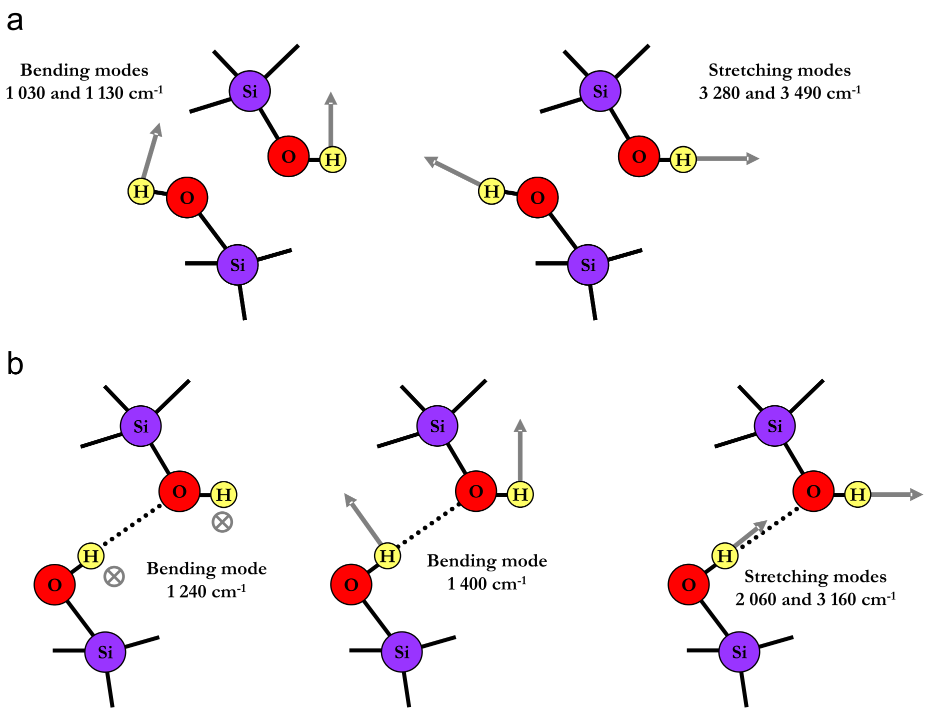

Fig. 4. Schematic synoptic of the highest vibration modes for both configurations (a) and (b).

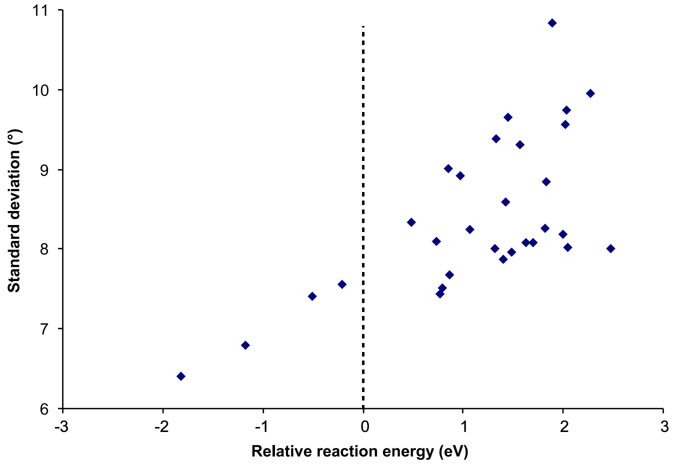

Fig. 5. Standard deviation of the distribution of final O–Si–O angles after structural optimizations as a function of their energy configurations.

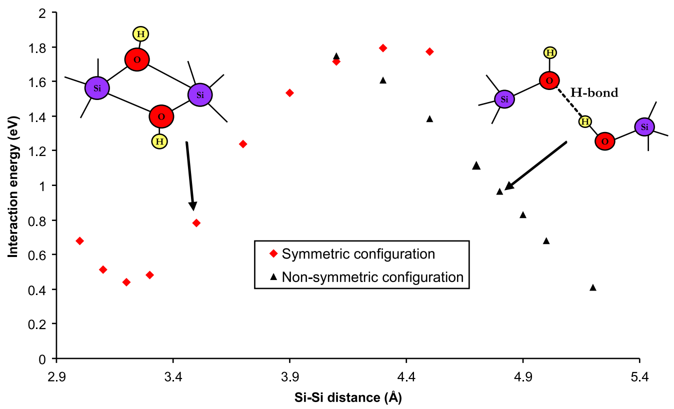

Fig. 6. Energies of to hydrolyzed configurations types as a function of Si–Si distance (Å).

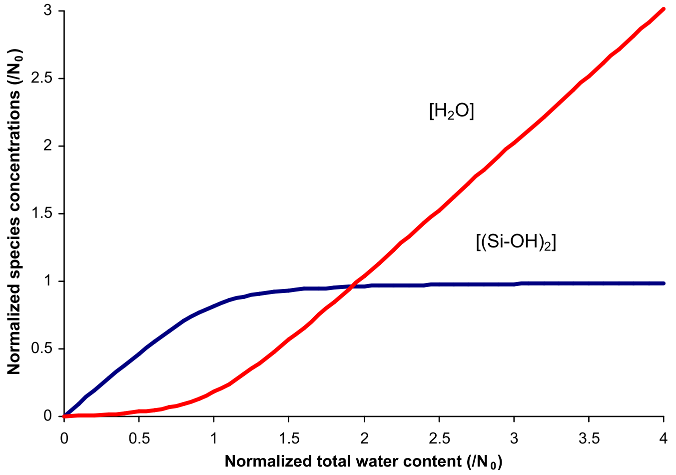

Fig. 7. Water speciation in glasses (*s* and *h* quantities, see text) according to Eq. (4) with $b=0.04$.

frequency proves that this is an effective bond; other studies, especially water adsorbed on different surfaces types (see Henderson [49]), refer to this kind of vibration as “rocking libration” with an eigenfrequency between 700 and 900 cm^{-1}. To check the stability of the structure and the bond strength, we have done an ab initio molecular dynamics calculation at $T=1000$ K during 1 ps: no change of the geometry has been observed.

In other Si–O–Al cases, the same behavior has been found as for the Si–O–Si bonds by optimizing all hydrolyzed bonds of the sample: symmetric as well as non-symmetric configurations have been obtained (see Figs. 11 and 12). In some cases, the non-symmetric structures after optimization lead to two kinds of structures, with a wide opening Al–O–Si bond; the final Al–Si distance can reach 4.2–4.5 Å. The favorable configurations (see Fig. 11) correspond to exothermic reactions, with a gain that varies from bond to bond and might reach 2.5 eV. All these calculations show that “active” sites exist even on Al–O–Si bonds,

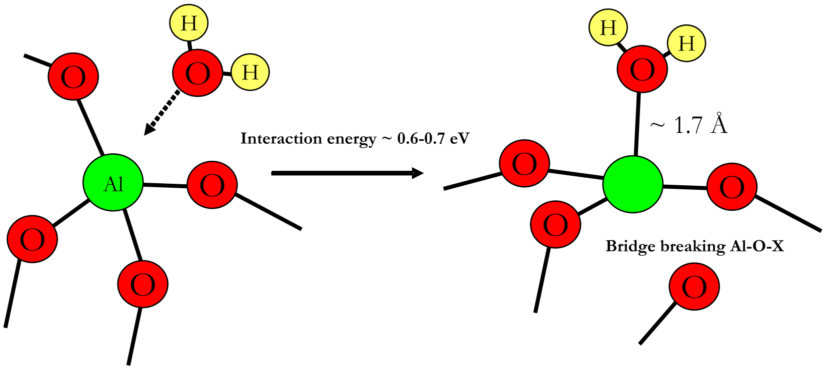

Fig. 8. AlO_3–H_2O species structure.

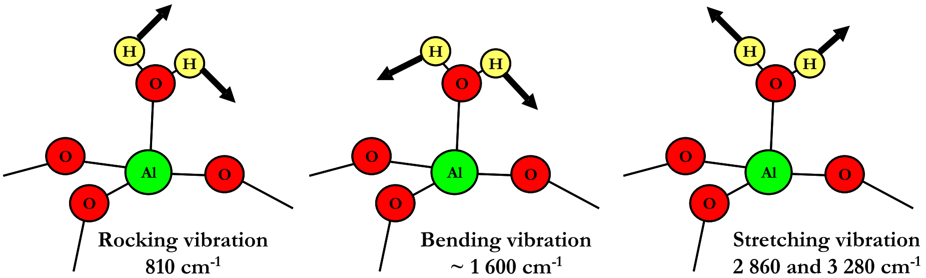

Fig. 9. AlO_3–H_2O vibrational modes: schematic representation of most significant four frequencies corresponding to the structure depicted in Fig. 8.

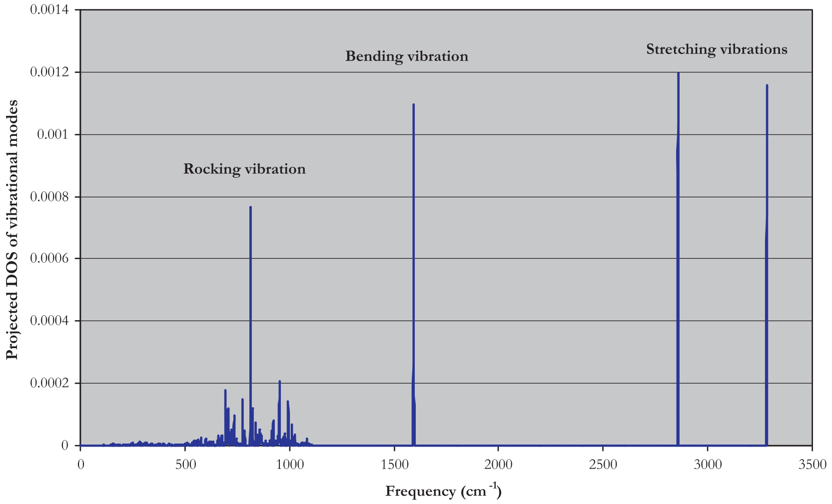

Fig. 10. Density of states (DOS) projected on H atoms of vibrational modes of the AlO_3–H_2O species structure (see Figs. 8 and 9).

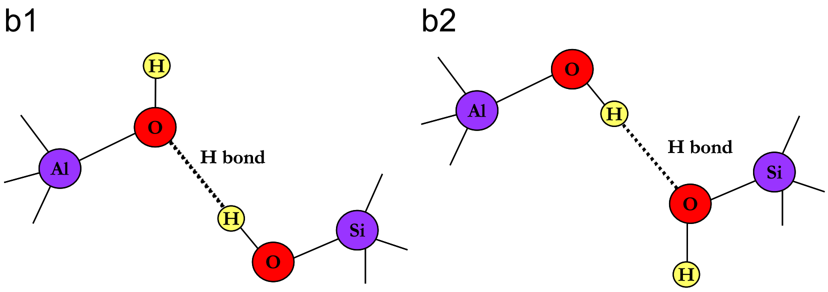

Fig. 11. Structures obtained after the hydrolysis of Al–O–Si bonds. The (b1) and (b2) configurations are those of the stable structures (exothermic processes within the glass bulk).

as the result of exoenergetic chemical processes. The structures obtained are two chemical groups Si–OH and Al–OH (silanol and aluminol groups) stabilized each other by an hydrogen bond.

3.5. *Model and discussions on the processes reactivity of Si–O–Al bond*

For further discussion, all these results suggest that silanol (Si–OH), aluminol (Al–OH) and Al–OH_2 groups are the products of hydrolysis into the aluminosilicates. Interactions may exist between Si–OH groups in front of Al–OH group. To test the stability of the resulting configurations, molecular dynamics simulations were performed over 1 ps at high temperature (1000 K). As depicted on Fig. 13, the reaction pathway shows a continuous round-trip of the H proton, until an exchange of protons occurs in order to form the Si–OH–Al entity. This H-exchange leaves a non-bridging oxygen in the cluster. It suggests that the Si–O–Al compound is more basic than Si–O–Si, which is in good agreement with experimental results in albite glasses [16].

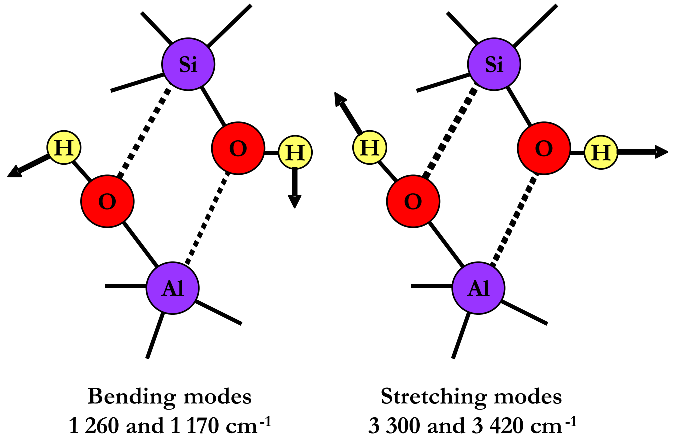

Fig. 12. Structures of an endoenergetic configuration after hydrolyzing Al–O–Si bonds and the four highest-frequency vibration modes.

The same mechanism was observed in an other way, through a structural optimization of a Si–O–Si bond. This hydrolysis produces two silanols groups, whose one switches and replaces the bridging oxygen of a near Al–O–Si bond (see Fig. 14). During this typical process, it is clear that the Ca counter cation changes from a compensator role to a network modifier one. The global mechanisms, underlied by this explicit exchange of the cation role, was suggested by Burnham [50] in 1975 in aluminosilicates glasses (see also [33]), and can be expressed as

$$M^{n+}(\mathrm{Al-O-Si})+\mathrm{Si-O-Si}+\mathrm{H_2O}\rightarrow \mathrm{Al-OH-Si}+\mathrm{Si-OH}+\mathrm{Si-O^-}\cdots M^+$$

where M^{n+} is the counter cation, with $n=1$ (Na^+) in the case of albitic glasses [50] and $n=2$ (Ca^{2+}) in the present work. In the products of this mechanism, the counter cation is becoming a network modifier, partially for a divalent ion, and completely for a monovalent ion. A non-bridging oxygen is leaved at the end of the process, and the Ca cation is less bounded to the network as it was in position of a charge compensator. This suggests a diffusion mechanism of the counter cation during the first step of hydrolysis processes within glasses (see [21,51,52]).

Towards the stability of the Al-OH group, let us return to a very simple quantum explanation. The Si–O–Si bonds are completely fulfilled; the $(SiO)_2$ group can be viewed in a simple manner

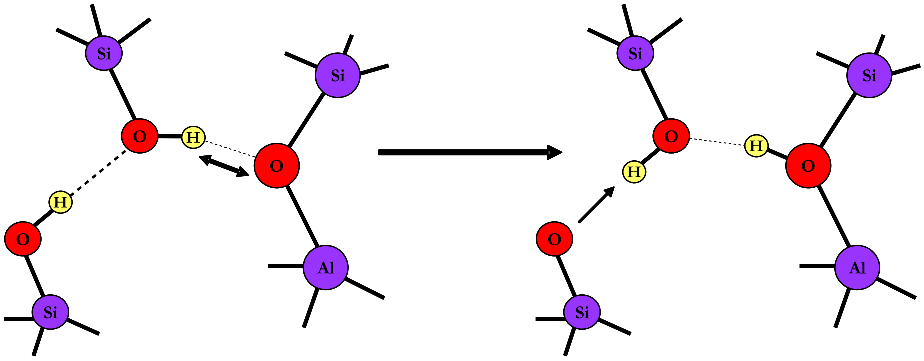

Fig. 13. Mechanism involving Si–OH, Al–OH, Si–OH–Al groups within aluminosilicates glasses (through ab initio molecular dynamics): formation of the Si–OH–Al entity coupled with an H exchange.

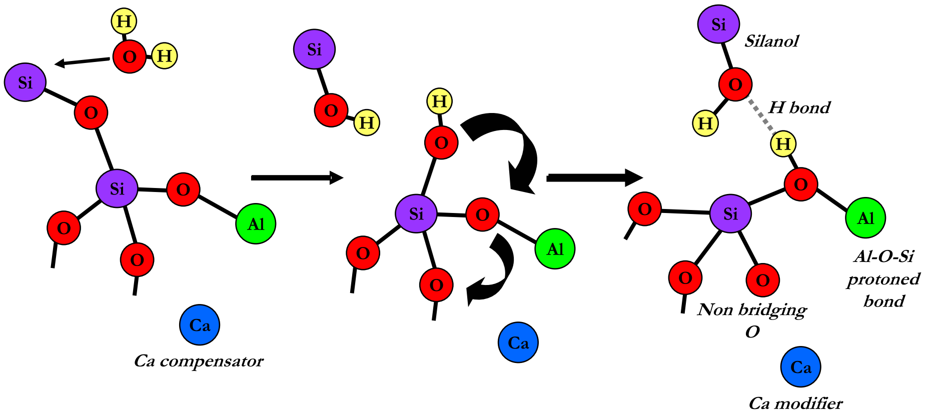

Fig. 14. Mechanism involving Si–OH, Al–OH, Si–OH–Al groups within aluminosilicates glasses (process determined through a structural optimization).

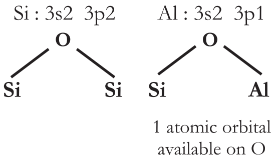

Fig. 15. Towards the Si–OH–Al stability (O has the 2s2 and 2p4 electronic configuration).

(Fig. 15) as well as the (Si–O–Al) cluster in terms of vacant or non-available atomic orbitals.

Compared to the Si–O–Si group (SiO_2 is a neutral species), the Si–O–Al entity has an atomic orbital available on the Oxygen atom, that can form a bond with a proton or a hydronium ion (H^+ or H_3O^+). Without forgetting that we are in condensed matter, only a part of an atomic orbital is available from a chemical point of view: for this reason, a new weak bond (not a strong covalent one, or shared bond with other atoms in the near neighborhood) is formed with the hydronium entity, as evidenced by the vibrational analysis, and especially the Al–OH frequency around $810\,cm^{-1}$. This simple interpretation might explain a diffusion process of molecular or dissociated water (via hydronium ion) into the glass bulk.

4. Conclusions

In the present work, mechanisms related to the reactivity of water into (calcium aluminosilicate CAS) glass bulk have been investigated by applying first principles techniques, *i.e.* DFT computations, with the use of the generalized gradient approximation (GGA) for the exchange and correlation term of the Kohn–Sham equations (Becke–Lee–Yang–Parr). It has been found that hydrolysis takes place only at specific sites (corresponding to exothermic sites) due to the amorphous character of the glass. After the hydrolysis, two silanols facing each other are formed and are stabilized by an hydrogen bond.

In aluminosilicates, the exoenergetic hydrolysis reactions tend to form Si–OH and Al–OH–Si entities. This kind of hydrolysis reaction can be the start point of a hydrogen diffusion process, in which the H-atom may jump from Al–O–Si to Al–O–Si bridges into the aluminosilicate glass bulk, as observed in two cases in our simulations. Moreover, a AlO_3–H_2O entity can be formed. The whole mechanism participates to the depolymerization of the vitreous network, one bridging oxygen (NBO) appearing into the glass: the charge compensator cation near the Al atom changes its role into a network modifier.

This study underlines the possible coupling between hydrolysis phenomena and interdiffusion mechanisms that occur into the glass at the first step of the leaching process (the hydrolysis steps have been very often and widely presented; for instance, the reader can refer to the bibliography of [53,51]). In borosilicates for example, the charge compensator cations do not diffuse with the same diffusion coefficient [54] as the network modifier ions: it suggests that these two cations types interact differently within the glass; the evolution from charge compensator into network modifier would necessary influence interdiffusion processes involving protons and sodium ions [18–20]. This is also what we suggest in a previous work [21] which focused on B–O–Si bonds hydrolysis and pointed out diffusion processes and ionic exchanges into borosilicate glasses. In contrast, in aluminosilicates, cationic charge compensators are retained into the bulk [55,24] and do not exchange with hydronium ions as easily as network cationic modifiers. Two mechanisms are in competition: molecular water diffusion H_2O onto non-reactives sites (and may form AlO_3–H_2O entity) or pass through aluminosilicates rings, hydrolysis reactions on reactive sites that open bonds and constrained rings. Both could occur, and if sufficient hydrolysis reactions have taken place, the former one could decrease the energy barrier necessary for water progression into the bulk by diffusion. This coupling of the phenomena could be a new explanation for the experimental results obtained by Smets and Lommen [23,56] in aluminosilicates glasses.

In perspective, one could therefore understand that the amorphous character of the glass might influence the reactivity of regular sites due to the short-range and mid-range structural disorder near each site; the question of the hydrolysis process remains after one reaction at a reactive site has occurred: the structure has been changed and some sites could therefore become reactive or non-reactive after this first hydrolysis (the structure relaxes around the hydrolyzed site). This is the reason why we are looking forward to access to the reactivity of glass by taking into account more than one water hydrolysis reaction at the same time or as the starting point configuration. Concerted reactions as well as changes of the mid-range structure might occur in the glass system which could change our chemical point of view of the global hydrolysis mechanism.

Acknowledgments

The authors want to acknowledge gratefully the whole team of the LCLT laboratory (J.-M. Delay, J.-E. Lartigue, P. Frugier, P. Jollivet and S. Gin) for fruitful discussions and advices along the theoretical study. They also are grateful to the whole CCRT team (Centre de Recherche et Technologie of the CEA) for their help in setting up codes on the CCRT clusters and for the whole support it provides.

References

[1] E. Vernaz, J. Dussossoy, Applied Geochemistry 7 (Suppl. 1) (1992) 13–22 (Geochemistry of Radioactive Waste Disposal: A French Contribution, ISSN 0883-2927).

[2] A. Ledieu, F. Devreux, P. Barboux, L. Sicard, O. Spalla, Journal of Non-Crystalline Solids 343 (1–3) (2004) 3–12 ISSN 0022-3093.

[3] A. Ledieu, F. Devreux, P. Barboux, Journal of Non-Crystalline Solids 345–346 (2004) 715–719 ISSN 0022-3093.

[4] F. Devreux, A. Ledieu, P. Barboux, Y. Minet, Journal of Non-Crystalline Solids 343 (1–3) (2004) 13–25 ISSN 0022-3093.

[5] B. Grambow, A general rate equation for nuclear waste glass corrosion, in: C. Jantzen, J. Stone, R. Ewing (Eds.), Scientific Basis for Nuclear Waste Management VII, vol. 44, Materials Research Society, Pittsburgh, PA1985, pp. 15–27.

[6] P. Frugier, C. Martin, I. Ribet, T. Advocat, S. Gin, Journal of Nuclear Materials 346 (2–3) (2005) 194–207 ISSN 0022-3115.

[7] P. Jollivet, G. Parisot, Journal of Nuclear Materials 345 (1) (2005) 46–64 ISSN 0022-3115.

[8] M. Heggie, R. Jones, Philosophical Magazine Letters 55 (1) (1987) 47–51.

[9] Y.T. Xiao, A.C. Lasaga, Geochimica Et Cosmochimica Acta 58 (24) (1994) 5379–5400.

[10] T. Bakos, S.N. Rashkeev, S.T. Pantelides, Physical Review Letters 88 (5) (2002) 055508/1–055508/4.

[11] J. Acocella, M. Tomozawa, E.B. Watson, Journal of Non-crystalline Solids 65 (2–3) (1984) 355–372.

[12] M. Tomozawa, Journal of Non-crystalline Solids 73 (1–3) (1985) 197–204.

[13] K.M. Davis, M. Tomozawa, Journal of Non-crystalline Solids 185 (3) (1995) 203–220.

[14] K.M. Davis, M. Tomozawa, Journal of Non-Crystalline Solids 201 (3) (1996) 177–198.

[15] A. Oehler, M. Tomozawa, Journal of Non-Crystalline Solids 347 (1–3) (2004) 211–219.

[16] L. Silver, E. Stolper, Journal of Petrology 30 (3) (1989) 667–709.

[17] B.C. Bunker, Journal of Non-Crystalline Solids 179 (1994) 300–308 ISSN 0022-3093.

[18] Z. Boksay, G. Bouquet, S. Dobos, Physics and Chemistry of Glasses 8 (4) (1967) 140–144.

[19] Z. Boksay, G. Bouquet, S. Dobos, Physics and Chemistry of Glasses 9 (2) (1968) 69–71.

[20] R.H. Doremus, Journal of Non-Crystalline Solids 19 (December) (1975) 137–144.

[21] G. Geneste, F. Bouyer, S. Gin, Journal of Non-Crystalline Solids 352 (28–29) (2006) 3147–3152.

[22] K.H. Schnatter, R.H. Doremus, W.A. Lanford, Journal of Non-Crystalline Solids 102 (1–3) (1988) 11–18.

[23] B.M.J. Smets, T.P.A. Lommen, Physics and Chemistry of Glasses 23 (3) (1982) 83–87.

[24] J.P. Hamilton, C.G. Pantano, Journal of Non-Crystalline Solids 222 (1997) 167–174.

[25] W.A. Lanford, K. Davis, P. Lamarche, T. Laursen, R. Groleau, R.H. Doremus, Journal of Non-Crystalline Solids 33 (2) (1979) 249–266.

[26] C.A. Houser, J.S. Herman, I.S.T. Tsong, W.B. White, American Ceramic Society Bulletin 58 (3) (1979) 376.

[27] I.S.T. Tsong, C.A. Houser, W.B. White, A.L. Winterberg, P.D. Miller, C.D. Moak, Applied Physics Letters 39 (8) (1981) 669–670.

[28] J.C. Dran, G. DellaMea, A. Paccagnella, J.C. Petit, L. Trotignon, Physics and Chemistry of Glasses 29 (6) (1988) 249–255.

[29] S.C. Kohn, R. Dupree, M.E. Smith, Geochimica Et Cosmochimica Acta 53 (11) (1989) 2925–2935.

[30] D. Sykes, J.D. Kubicki, Geochimica Et Cosmochimica Acta 57 (5) (1993) 1039–1052.

[31] S.C. Kohn, R. Dupree, M.G. Mortuza, Chemical Geology 96 (3–4) (1992) 399–409.

[32] S.C. Kohn, M.E. Smith, P.J. Dirken, E.R.H. van Eck, A.P.M. Kentgens, R. Dupree, Geochimica Et Cosmochimica Acta 62 (1) (1998) 79–87.

[33] S.C. Kohn, Mineralogical Magazine 64 (3) (2000) 389–408.

[34] R.H. Doremus, Journal of Non-Crystalline Solids 55 (1) (1983) 143–147.

[35] J.V. Oglesby, J.F. Stebbins, American Mineralogist 85 (5–6) (2000) 722–731.

[36] Y. Liu, H. Nekvasil, H.B. Long, Geochimica Et Cosmochimica Acta 66 (23) (2002) 4149–4163.

[37] J.D. Kubicki, D.G. Sykes, Geochimica Et Cosmochimica Acta 68 (19) (2004) 3909–3918.

[38] P. Ganster, Modélisation des verres intervenant dans le conditionnement des déchets radioactifs par dynamique moléculaires classique et AB initio, Ph.D. Thesis, Université de Montpellier II, 2004.

[39] P. Ganster, M. Benoit, W. Kob, J.M. Delaye, Journal of Chemical Physics 120 (21) (2004) 10172–10181.

[40] D. SanchezPortal, P. Ordejon, E. Artacho, J.M. Soler, International Journal of Quantum Chemistry 65 (5) (1997) 453–461.

[41] J.M. Soler, E. Artacho, J.D. Gale, A. Garcia, J. Junquera, P. Ordejon, D. Sanchez-Portal, Journal of Physics: Condensed Matter 14 (11) (2002) 2745–2779.

[42] N.A. Spaldin, W.E. Pickett, Journal of Solid State Chemistry 176 (2) (2003) 615–632 . doi:10.1016/j.jssc.2003.07.001 Special issue on The Impact of Theoretical Methods on Solid-State Chemistry, ISSN 0022-4596.

[43] W. Kohn, L.J. Sham, Physical Review 140 (4A) (1965) A1133–A1138.

[44] A.D. Becke, Physical Review A 38 (6) (1988) 3098–3100.

[45] C.T. Lee, W.T. Yang, R.G. Parr, Physical Review B 37 (2) (1988) 785–789.

[46] N. Troullier, J.L. Martins, Physical Review B 43 (3) (1991) 1993–2006.

[47] N. Troullier, J.L. Martins, Physical Review B 43 (11) (1991) 8861–8869.

[48] F. Bouyer, From first-principles computations to thermochemical determinations: a way to assess ab initio calculations basis, 2010.

[49] M.A. Henderson, Surface Science Reports 46 (1–8) (2002) 5–308.

[50] C.W. Burnham, Geochimica Et Cosmochimica Acta 39 (8) (1975) 1077–1084.

[51] L. Chomat, F. Bouyer, S. Gin, Modelling the leaching of fractured SON 68 glass block, in: XXIeme International Congress on Glass (ICG2007), Strasbourg, 2007.

[52] P. Frugier, S. Gin, Y. Minet, T. Chave, B. Bonin, N. Godon, J.-E. Lartigue, P. Jollivet, A. Ayral, L.D. Windt, G. Santarini, Journal of Nuclear Materials 380 (1–3) (2008) 8–21 ISSN 0022-3115.

[53] P. Frugier, T. Chave, S. Gin, J.-E. Lartigue, Journal of Nuclear Materials 392 (3) (2009) 552–567 ISSN 0022-3115.

[54] A. Grandjean, M. Malki, C. Simonnet, Journal of Non-crystalline Solids 352 (26–27) (2006) 2731–2736.

[55] W. Smit, H.N. Stein, Journal of Non-Crystalline Solids 34 (3) (1979) 357–370.

[56] B.M.J. Smets, T.P.A. Lommen, Journal De Physique 43 (NC-9) (1982) 649–652.